



## Measurements with an ultrafast scanning tunnelling microscope on photoexcited semiconductor layers

Keil, Ulrich Dieter Felix; Jensen, Jacob Riis; Hvam, Jørn Märcher

*Published in:*

Lasers and Electro-Optics, 1998. CLEO 98. Technical Digest. Summaries of papers presented at the Conference on

*Link to article, DOI:*

[10.1109/CLEO.1998.676142](https://doi.org/10.1109/CLEO.1998.676142)

*Publication date:*

1998

*Document Version*

Publisher's PDF, also known as Version of record

[Link back to DTU Orbit](#)

*Citation (APA):*

Keil, U. D. F., Jensen, J. R., & Hvam, J. M. (1998). Measurements with an ultrafast scanning tunnelling microscope on photoexcited semiconductor layers. In *Lasers and Electro-Optics, 1998. CLEO 98. Technical Digest. Summaries of papers presented at the Conference on* (pp. 262-263). IEEE. <https://doi.org/10.1109/CLEO.1998.676142>

---

### General rights

Copyright and moral rights for the publications made accessible in the public portal are retained by the authors and/or other copyright owners and it is a condition of accessing publications that users recognise and abide by the legal requirements associated with these rights.

- Users may download and print one copy of any publication from the public portal for the purpose of private study or research.
- You may not further distribute the material or use it for any profit-making activity or commercial gain
- You may freely distribute the URL identifying the publication in the public portal

If you believe that this document breaches copyright please contact us providing details, and we will remove access to the work immediately and investigate your claim.

Wednesday, May 6

GaAs photonconductive dipole antenna for generation of a radiation with a frequency corresponding to the mode separation of the LD. Due to the common-mode rejection effect of the identical laser cavity, the spectral linewidth of the generated radiation is approximately more than two times narrower compared with that of each mode of the LD. We used a simultaneous two-mode-oscillation distributed Bragg reflector (DBR) laser with a two-frequency feedback grating, which operated at 851 nm and excited LTG-GaAs photomixer at room temperature. A stable two-mode operation was achieved by adjusting the bias current and the operating temperature of the laser. Figure 1 shows the spectrum of the two-mode LD at 191 mA bias current and 19 °C measured by using a double-monochromator. The difference of the frequency between the two modes is 0.39 nm (163.5 GHz). The spectral width, estimated by using a scanning Fabry-Perot with 50 MHz resolution, was 240 MHz.

The experimental setup was similar to that used in the experiment of Tani *et al.*<sup>3</sup> The two-mode laser beam (10 mW) was focused on the 5- $\mu\text{m}$  gap, which was biased with 40 V of 1-mm-long dipole antenna fabricated on the LTG-GaAs. The radiation was led into a Martin-Puplett polarizing interferometer with a 0.8-GHz spectral resolution. The interference signal measured with an InSb hot-electron bolometer at 4.2 K is shown in Fig. 2, where the inset is a fast Fourier transform (FFT) of the interferogram. Generation of radiation with the same frequency as the beat frequency of the two-mode LD (Fig. 1) indicates that the radiation from the antenna originates from a modulated current by the laser. From the decay of the interferometric component against the averaged detected power with increasing path difference shown in Fig. 2, we estimated the coherent length of the radiation to be larger than 230 cm. This indicates that the linewidth of the radiation is smaller than 130 MHz, confirming the common-mode rejection effect, by which a large part of the frequency fluctuations of the two laser modes is canceled out, and the beat frequency of the laser is stabilized as has been demonstrated in Hyodo *et al.*<sup>4</sup>

In conclusion, it was demonstrated that the identical laser cavity effectively suppressed common-mode frequency fluctuation and the two-longitudinal-mode laser is an excellent source for sub-THz wave generation by photo-mixing.

\*Department of Electric Engineering, Shonan Institute of Technology, 1-1-25 Tujido-Nishikaigan, Fujizawa, Kanagawa 251, Japan

1. E.R. Brown *et al.*, Appl. Phys. Lett. **66**, 285 (1995).
2. S. Matsuura *et al.*, Appl. Phys. Lett. **70**, 3844 (1997).
3. M. Tani *et al.*, IEEE Microwave Guided Wave Lett. **7**, 282 (1997).
4. M. Hyodo *et al.*, Electron. Lett. **33**, 1589 (1996).

**CWF51**

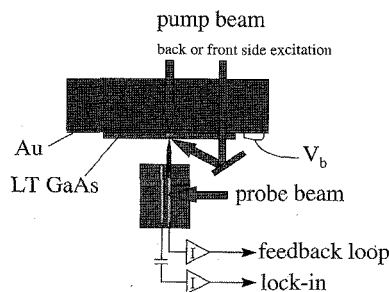
**Measurements with an ultrafast scanning tunneling microscope on photoexcited semiconductor layers**

Ulrich D. Keil, Jacob R. Jensen, Jørn M. Hvam, *Mikroelektronik Centret, DTU Building 345 east, DK-2800 Lyngby, Denmark; E-mail: ulli@mic.dtu.dk*

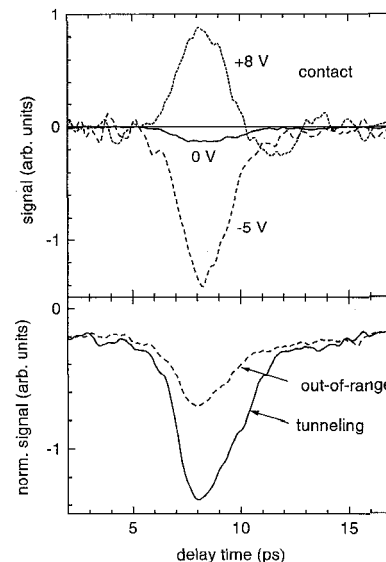
Thus far, the photoconductively gated ultrafast scanning tunneling microscope (USTM) has only been demonstrated on transmission lines.<sup>1-3</sup> We extend the use of the USTM to resolve field transients on semiconductor layers. The laser pump beam generates carriers in the semiconductor layer; the probe beam gates the signal picked up by the tunneling tip. The photoconductive (PC) switch connected to the tunneling tip is illuminated through a fiber with a 100-fs Ti:sapphire laser. The sample consists of a 1.5- $\mu\text{m}$ -thick layer of low-temperature (LT) grown GaAs. The LT GaAs layer is lifted off from the GaAs substrate and placed on a transparent substrate with a semi-transparent Au-layer (Fig. 1). The transparent substrate allows for illumination from the back (Au) side as well as from the front (tip) side.

The measurement (Fig. 2, top) with the tip in contact to the substrate is a measure of the transient photocurrent and serves as a reference for the measurement in tunneling mode. The pulse width of about 2 ps is determined by the carrier lifetime of the LT GaAs layer. In order to operate the instrument reasonably stable in constant current mode, a tunneling current of 50 pA is chosen, approximately 100 smaller than in contact. At the bottom of Fig. 2, the transient measurement with the tip in tunneling mode and at a distance of around 1  $\mu\text{m}$  are compared. The tunneling mode signal follows in shape and sign the contact measurement for negative bias, while the amplitude drops by a factor of 6. The fact that a signal is measured out of the tunneling range indicates that the signal is capacitively coupled to the tunneling tip. Capacitive coupling has been identified as the coupling mechanism for measurements on transmission lines.<sup>2,4</sup>

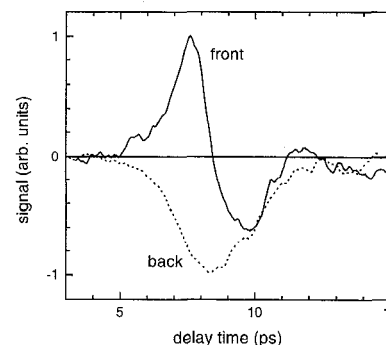
The sign of the tunneling mode transient can be explained by the nonuniform carrier profile excited by the laser. If we neglect the hole contribution to the current, we expect an electron diffusion current towards the tip (in excitation direction) as the dominating contri-



**CWF51 Fig. 1.** Setup for the USTM on a semiconductor layer. The sample consists of a 1.5- $\mu\text{m}$  LT GaAs placed on a sapphire substrate with a 40-nm Au layer. The sample can be excited either from the back or the front side.



**CWF51 Fig. 2.** Back side excitation: transient photocurrent measurements in contact (top) and transient field measurements in tunneling mode and out of tunneling range (bottom).



**CWF51 Fig. 3.** Comparison of the transient signal in tunneling mode for back and front side excitation. Both signals are normalized independently.

tribution. The sign is equivalent to a drift current for a negative bias on the back side. Figure 3 shows that the signal is indeed strongly dependent on the excitation direction. For front side illumination the main contribution changes sign. Although the illumination via a mirror is more versatile, as it does not require a transparent substrate, it results in a more complicated photoinduced carrier profile. The carrier profile is determined by the incident angle and the tip shadow, which accounts for the more complicated signal shape.

In summary, we demonstrate the use of a USTM for detecting laser-induced field transients on semiconductor layers. In principle, the instrument can detect transient field changes thus far observed as far-field THz radiation in the near-field regime and resolve small signal sources. For photoexcited LT GaAs we can explain the signal by a diffusion current driven by the laser-induced carrier density gradient.

1. S. Weiss, D. Botkin, D.F. Ogletree, M. Salmeron, D.S. Chemla, Appl. Phys. Lett. **63**, 2567 (1993).

2. R.H.M. Groeneveld, H. van Kempen, Appl. Phys. Lett. **69**, 2294 (1996).
3. J.R. Jensen, U.D. Keil, J.M. Hvam, Appl. Phys. Lett. **70**, 2625 (1997).
4. U.D. Keil, J.R. Jensen, J.M. Hvam, Appl. Phys. Lett. **70**, (19), 2625 (1997).

**CWF52**

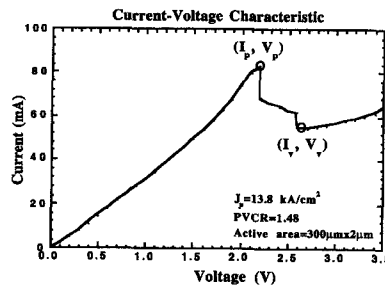
**Integration of a resonant tunneling diode and an optical waveguide to form an electroabsorption modulator with a large bandwidth to drive voltage ratio**

J.M.L. Figueiredo,\* A.M.P. Leite,\*\* C.R. Stanley, C.N. Ironside, *Department of Electronics and Electrical Engineering, University of Glasgow, Glasgow, G12 8LT, United Kingdom*

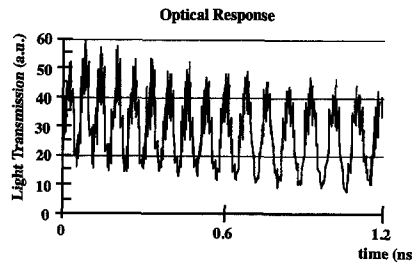
Traditionally, electroabsorption optical modulators have operated by reverse biasing a p-n junction. Here, we present an entirely new approach of employing the electrical characteristics of a resonant tunneling diode (RTD) to switch an electrical field within an optical waveguide. A key advantage is that by correct dc biasing, the device can provide high bandwidth electrical gain for the drive signal of the modulator; thereby the modulator can have an exceptionally high bandwidth to drive voltage ratio. Moreover, the RTD electrical properties can provide oscillation and harmonic multiplication at high frequency.

Employing the RTD for high-speed electroabsorption modulation was investigated using the device configuration illustrated in Fig. 1, which shows the integration of a RTD with an optical waveguide. The electrical properties (see Fig. 2), introduced by the RTD into the optical waveguide, give the capability of easily switching large electric fields in the collector region by dc biasing in the negative differential resistance region of the *I-V* curve. A small rf drive signal then causes peak-to-valley switching that results in a band-edge shift via the Franz-Keldysh effect;<sup>1</sup> thereby producing electroabsorption modulation for light at photon energies close to the bandgap energy of the semiconductor, in this case around 900 nm. When dc biased in the negative differential resistance region of the *I-V* curve, the device has wideband electrical gain and allows efficient high-speed intensity modulation requiring a few hundred millivolts as RF drive voltage.

The RTD waveguide transmission spectrum was measured at zero bias, at the peak, and at the valley using light from a tuneable Ti:sapphire laser. The observed shift on the



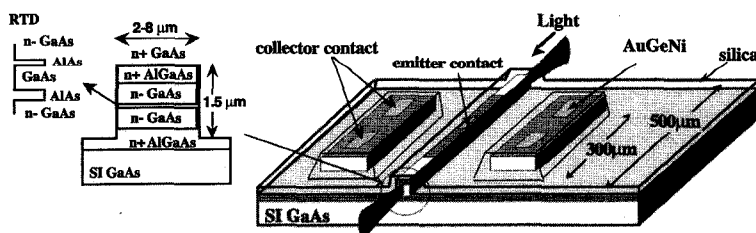
CWF52 Fig. 2. Current-voltage characteristic for a 2 μm × 300 μm active area RTD optical waveguide modulator. The device shows negative differential resistance in the bias voltage range 2.2–2.6V.



CWF52 Fig. 3. Streak camera measurements of the 6 dB @ 14 GHz optical response of a 2 μm × 300 μm active area RTD optical waveguide modulator from 0.4 V @ 958 MHz drive signals. The packaged device was dc biased at approximately 2.4 V.

spectrum at the RTD resonance was 15 nm. The band edge shifted when biased at the valley was around 23 nm. To investigate the high-frequency optical response of the packaged device, a streak camera was used to detect the optical signal. The device was dc biased in the negative differential region. The dc and the rf signal were applied through a bias tee. The packaged device shows electrical gain at a resonance around 14 GHz and can lock in to high harmonics of an applied signal around 1 GHz. We have observed 6-dB modulation depth around 14 GHz for an applied voltage 0.4 V @ 1 GHz, implying a bandwidth-to-voltage ratio of 33 GHz/V @ 6 dB. The streak camera measurement of the 14-GHz optical modulation due to a 0.4 V @ 958-MHz signal is presented in Fig. 3.

We have demonstrated a new device concept; by introducing an RTD to an optical waveguide an electroabsorption modulator can be integrated with a high bandwidth elec-



CWF52 Fig. 1. RTD optical waveguide modulator schematic diagram before the 50 Ω coplanar waveguide transmission line definition and the wafer schematic diagram.

trical amplifier. The results are an early indication that the device does have a large bandwidth-to-drive-voltage ratio due to the electrical gain and a large modulation bandwidth. The device can be further improved and extended to optical communication wavelengths. We are presently investigating a device implemented on a InAlGaAs/InP-based material system towards the 1550 nm operation, which could have higher bandwidth, higher bandwidth-to-drive-voltage ratio, and higher extinction ratio due to the better material characteristics, which give higher current density, higher peak-to-valley current ratio, and higher electron saturation velocity.<sup>2</sup>

\*Also with Centro de Fisica, University of Porto, Rua Campo Alegre 687, 4150 PORTO, Portugal.

\*\*Centro de Fisica, University of Porto, Rua Campo Alegre 687, 4150 PORTO, Portugal

1. S.G. McMeekin, M.R.S. Taylor, B. Vögele, C.R. Stanley, C.N. Ironside, Appl. Phys. Lett. **65**, 1076–1078 (1994).
2. T.P.E. Broekaert, C.G. Fonstad, J. Appl. Phys. **68**, 4310–4312 (1990).

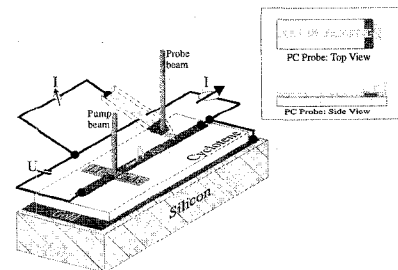
**CWF53**

**External photoconductive sampling up to 1 THz**

H.-M. Heiliger, G. Vortmeier, H. Kurz, *Institut für Halbleitertechnik II, Rheinisch-Westfälische Technische Hochschule Aachen, Sommerfeldstr. 24, D-52056 Aachen, Germany*

Photoconductive (PC) sampling is regarded as a powerful tool for characterization of ultrahigh-frequency electronic devices. However, up to now, mostly the detection of single pulses of fairly short duration around 2.3 ps have been shown.<sup>1–3</sup> Thus, there is real need to demonstrate the capability of this method for device characterization in the same way as for electro-optic (EO) sampling. Here, we present the characterization of a 50-Ω-impedance thin-film microstrip line (TFMSL) by means of an external PC probe. The results for the attenuation α(f) and the effective permittivity ε<sub>r,eff</sub>(f) (f: frequency) are compared up to 1 THz with the data extracted from EO measurements employing identically fabricated lines of the same dimensions.

The TFMSL, as sketched in Fig. 1, is prepared on low-resistivity (5–8 Ωcm) Si substrate. It consists of a 20/780-nm-thick Ti/Au ground conductor and a 20-mm-long, 7.4-μm-wide and 20/780-nm-thick Ti/Au signal



CWF53 Fig. 1. Schematic of the measurement setup for external PC sampling.

Wednesday, May 6